

Supporting Information

**Compositional evolution of the NaZn₁₃ structure motif in the systems
La–Ni–Ga and Ce–Ni–Ga**

Yurii Prots,^{*a} Leonid Vasylechko,^b Wilder Carrillo-Cabrera,^a Christina Drathen,^c Mauro Coduri,^c
Dariusz Kaczorowski,^d Ulrich Burkhardt,^a Yuri Grin^{*a}

^a*Max-Planck-Institut für Chemische Physik fester Stoffe, Nöthnitzer Str. 40, 01187 Dresden,
Germany*

^b*Lviv Polytechnic National University, 12 Bandera St., 79013 Lviv, Ukraine*

^c*ESRF - the European Synchrotron, 71, Avenue des Martyrs, 38000 Grenoble, France*

^d*Institute of Low Temperature and Structure Research, Polish Academy of Sciences, ul. Okólna
2, 50-422 Wrocław, Poland*

Table S1 Crystallographic data of the $\text{LaNi}_{13-x}\text{Ga}_x$ samples ($2 \leq x \leq 8$)^a

Nominal composition	Space group, (phase amount, wt. %)	a , Å	b , Å	c , Å	V_c , Å ³
$\text{LaNi}_{11}\text{Ga}_2$ ^b	$Fm\bar{3}c$ (87 %)	11.3941(4)	–	–	1479.3(1)
$\text{LaNi}_{10.5}\text{Ga}_{2.5}$ [*]	$I4/mcm$	8.05099(7)	–	11.4888(2)	1489.38(6)
$\text{LaNi}_{10}\text{Ga}_3$	$I4/mcm$	8.0508(4)	–	11.5750(6)	1500.6(2)
$\text{LaNi}_{9.75}\text{Ga}_{3.25}$	$I4/mcm$	8.0532(4)	–	11.6254(6)	1507.8(2)
$\text{LaNi}_{9.5}\text{Ga}_{3.5}$	$I4/mcm$	8.0541(4)	–	11.6471(6)	1511.0(2)
$\text{LaNi}_{9.25}\text{Ga}_{3.75}$	$I4/mcm$	8.0529(4)	–	11.6855(6)	1515.6(2)
LaNi_9Ga_4 [*]	$I4/mcm$	8.05861(3)	–	11.75707(7)	1527.04(2)
$\text{LaNi}_{8.75}\text{Ga}_{4.25}$ [*]	$I4/mcm$	8.0630(1)	–	11.7760(2)	1531.18(8)
$\text{LaNi}_{8.63}\text{Ga}_{4.37}$ [*]	$I4/mcm$	8.06763(9)	–	11.7903(2)	1534.78(6)
$\text{LaNi}_{8.5}\text{Ga}_{4.5}$ [*]	$Ibam$	7.9270(3)	8.2221(3)	11.8117(4)	1539.7(2)
$\text{LaNi}_{8.25}\text{Ga}_{4.75}$ [*]	$Ibam$	7.8900(1)	8.2748(1)	11.8360(2)	1545.50(6)
LaNi_8Ga_5 [*]	$Ibam$	7.84446(7)	8.34335(7)	11.86514(9)	1553.12(4)
$\text{LaNi}_{7.75}\text{Ga}_{5.25}$ [*]	$Ibam$	7.82855(9)	8.38497(9)	11.8861(1)	1560.46(6)
$\text{LaNi}_{7.5}\text{Ga}_{5.5}$ [*]	$Ibam$	7.8268(1)	8.4150(2)	11.9041(2)	1568.06(8)
$\text{LaNi}_{7.25}\text{Ga}_{5.75}$ [*]	$Ibam$	7.82870(7)	8.43691(9)	11.9207(1)	1574.74(4)
$\text{LaNi}_{6.88}\text{Ga}_{6.12}$ [*]	$Ibam$ (73 %)	7.8443(3)	8.4503(4)	11.9309(6)	1581.8(2)
	$Fmmm$ (27%)	11.4520(1)	11.9053(9)	11.7147(9)	1597.2(4)
$\text{LaNi}_{6.75}\text{Ga}_{6.25}$ [*]	$Ibam$ (46 %)	7.8415(3)	8.4542(3)	11.9111(5)	1579.3(1)
	$Fmmm$ (54 %)	11.4473(3)	11.9043(3)	11.7136(3)	1596.3(2)
$\text{LaNi}_{6.63}\text{Ga}_{6.37}$ [*]	$Fmmm$	11.4537(2)	11.9004(2)	11.7218(2)	1597.72(8)
$\text{LaNi}_{6.5}\text{Ga}_{6.5}$ [*]	$Fmmm$	11.46196(9)	11.89553(8)	11.73591(8)	1600.15(4)
$\text{LaNi}_{6.25}\text{Ga}_{6.75}$ [*]	$Fmmm$	11.5604(2)	11.8387(2)	11.7711(2)	1611.00(6)
$\text{LaNi}_{6.13}\text{Ga}_{6.87}$ [*]	$Fmmm$	11.6294(1)	11.7870(2)	11.7871(2)	1615.71(7)
LaNi_6Ga_7 [*]	$I4/mcm$	8.28529(8)	–	11.8053(2)	1620.78(6)
$\text{LaNi}_{5.5}\text{Ga}_{7.5}$ [*]	$I4/mcm$	8.32050(2)	–	11.83597(4)	1638.83(1)
$\text{LaNi}_{5.25}\text{Ga}_{7.75}$ ^c	$I4/mcm$ (66 %)	8.3232(5)	–	11.8370(9)	1639.9(4)
LaNi_5Ga_8 ^c	$I4/mcm$ (56 %)	8.3226(5)	–	11.8380(9)	1639.8(4)

^a unit cell volumes (V_c) is normalized to the aristotype NaZn_{13} -type cubic cell as follow:

$$V_c = 2V_t (I4/mcm); V_c = 2V_o (Ibam); V_c = V_o (Fmmm);$$

^b neighboring phases: $\text{La}(\text{Ni}_{1-x}\text{Ga}_x)_5$ and Ni;

^c neighboring phases: $\text{La}(\text{Ni}_{1-x}\text{Ga}_x)_4 + \text{Ni}_2\text{Ga}_3$;

* X-ray synchrotron data (ID22 at ESRF).

Table S2 Crystallographic data of the CeNi_{13-x}Ga_x samples ($3 \leq x \leq 7.62$)^a

Nominal composition	Space group, (phase amount, wt. %)	<i>a</i> , Å	<i>b</i> , Å	<i>c</i> , Å	<i>V_c</i> , Å ³
CeNi ₁₀ Ga ₃ ^b	–	–	–	–	–
CeNi _{9.75} Ga _{3.25} ^b	<i>I4/mcm</i> (32 %)	8.036(1)	–	11.708(3)	1512.0(8)
CeNi _{9.5} Ga _{3.5} ^b	<i>I4/mcm</i> (69 %)	8.0360(7)	–	11.709(2)	1512.2(6)
CeNi _{9.25} Ga _{3.75} ^b	<i>I4/mcm</i> (83 %)	8.0347(3)	–	11.7074(6)	1511.6(2)
CeNi ₉ Ga ₄ ^b	<i>I4/mcm</i> (96 %)	8.0369(4)	–	11.7159(8)	1513.6(2)
CeNi _{8.75} Ga _{4.25} [*]	<i>I4/mcm</i>	8.04614(2)	–	11.75153(4)	1521.60(2)
CeNi _{8.5} Ga _{4.5} [*]	<i>Ibam</i>	7.9212(2)	8.1896(3)	11.7815(3)	1528.6(2)
CeNi _{8.25} Ga _{4.75} [*]	<i>Ibam</i>	7.84488(9)	8.28690(9)	11.8144(1)	1536.1(1)
CeNi ₈ Ga ₅	<i>Ibam</i>	7.8041(8)	8.3420(9)	11.836(2)	1541.2(6)
CeNi _{7.75} Ga _{5.25}	<i>Ibam</i>	7.7796(1)	8.3935(1)	11.8581(2)	1548.64(6)
CeNi _{7.5} Ga _{5.5}	<i>Ibam</i>	7.7792(5)	8.4273(5)	11.8809(8)	1557.8(4)
CeNi _{7.25} Ga _{5.75} [*]	<i>Ibam</i>	7.78328(6)	8.45196(6)	11.90233(9)	1565.96(4)
CeNi ₇ Ga ₆	<i>Ibam</i>	7.7937(7)	8.4641(7)	11.916(1)	1570.2(4)
CeNi _{6.88} Ga _{6.12}	<i>Ibam</i> (66 %)	7.808(4)	8.466(4)	11.905(7)	1573.8(9)
	<i>Fmmm</i> (34 %)	11.426(3)	11.872(3)	11.703(3)	1587.6(9)
CeNi _{6.75} Ga _{6.25} [*]	<i>Ibam</i> (10 %)	7.802(1)	8.469(2)	11.908(3)	1573.6(8)
	<i>Fmmm</i> (90 %)	11.4281(3)	11.8742(4)	11.7097(3)	1589.1(2)
CeNi _{6.63} Ga _{6.37}	<i>Fmmm</i>	11.424(2)	11.875(2)	11.700(2)	1587.3(8)
CeNi _{6.5} Ga _{6.5} [*]	<i>Fmmm</i>	11.42882(2)	11.87373(2)	11.71262(2)	1589.44(1)
CeNi _{6.25} Ga _{6.75}	<i>Fmmm</i>	11.5245(6)	11.8103(7)	11.7454(8)	1598.6(3)
CeNi _{6.13} Ga _{6.87} [*]	<i>Fmmm</i>	11.6092(3)	11.7489(4)	11.7659(3)	1604.8(1)
CeNi ₆ Ga ₇	<i>I4/mcm</i>	8.2629(4)	–	11.7866(8)	1609.4(4)
CeNi _{5.75} Ga _{7.25}	<i>I4/mcm</i>	8.2819(2)	–	11.8015(3)	1618.9(1)
CeNi _{5.63} Ga _{7.37}	<i>I4/mcm</i>	8.2864(7)	–	11.805(2)	1621.2(4)
CeNi _{5.5} Ga _{7.5} ^c	<i>I4/mcm</i> (52 %)	8.286(4)	–	11.804(8)	1621.0(9)
CeNi _{5.38} Ga _{7.62} ^c	<i>I4/mcm</i> (39 %)	8.286(2)	–	11.804(4)	1620.9(9)

^a unit cell volumes (*V_c*) is normalized to the aristotype NaZn₁₃-type cubic cell as follow:

$$V_c = 2V_t \text{ (} I4/mcm \text{)}; V_c = 2V_o \text{ (} Ibam \text{)}; V_c = V_o \text{ (} Fmmm \text{)};$$

^b neighboring phases: Ce(Ni_{1-x}Ga_x)₅ + Ni₃Ga;

^c neighboring phases: Ce(Ni_{1-x}Ga_x)₄ + Ni₂Ga₃;

* X-ray synchrotron data (ID22 at ESRF).

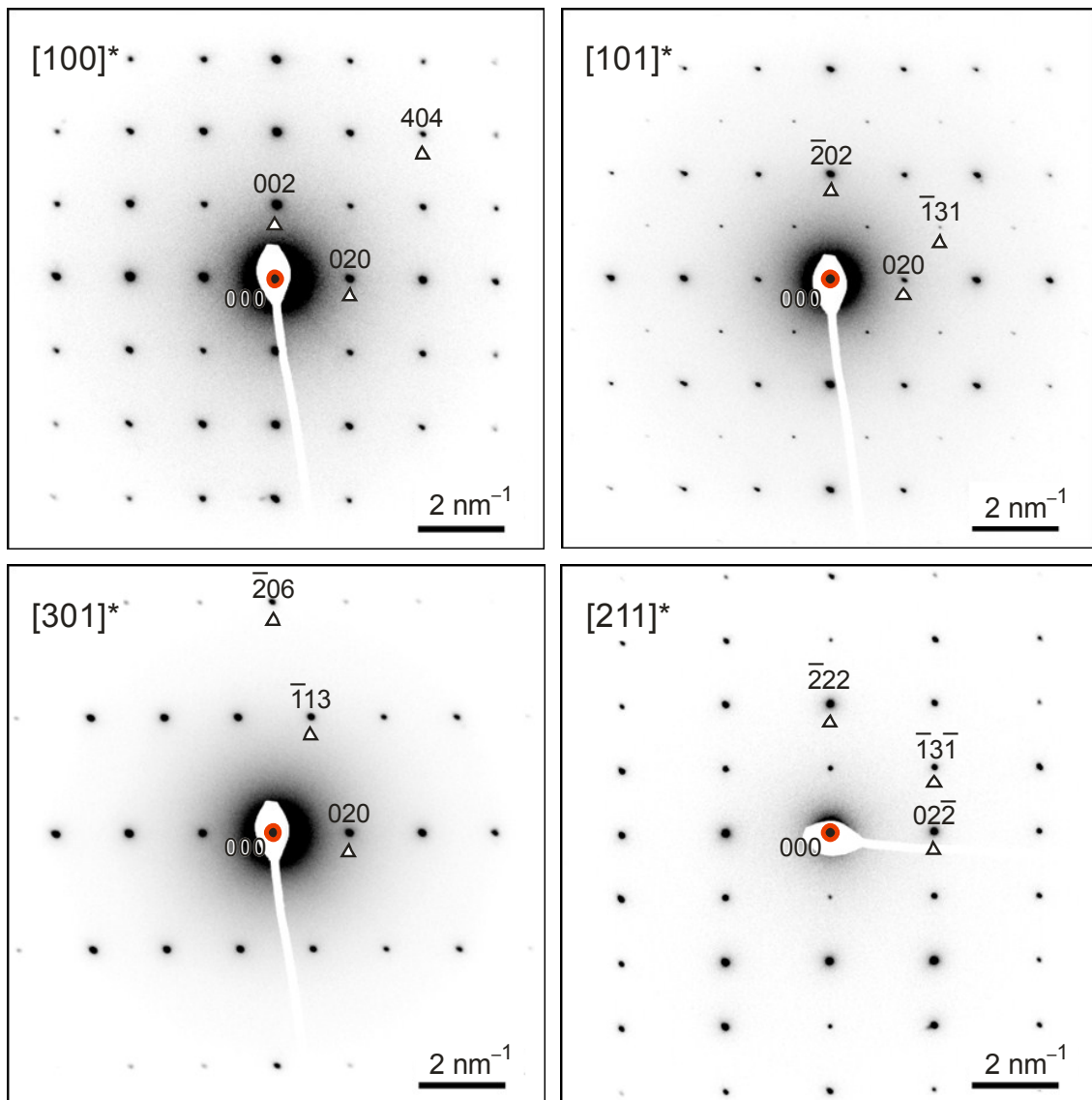


Figure S1. Selected area diffraction patterns of $\text{LaNi}_{6.5}\text{Ga}_{6.5}$ along $[100]^*$, $[101]^*$, $[301]^*$ and $[211]^*$ directions, showing that the crystal structure is F -centered.

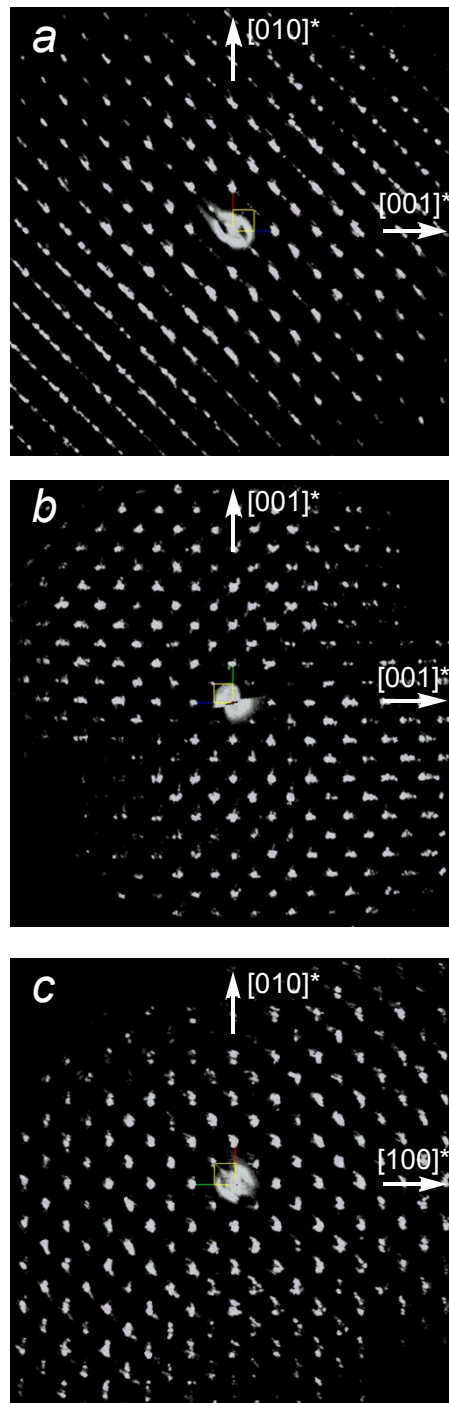


Figure S2. Projections of 3D diffraction pattern (reciprocal volume) for LaNi_{6.5}Ga_{6.5} sample along (a) [100], (b) [010] and (c) [001] directions. Extra reflections originate from neighboring twin crystal.

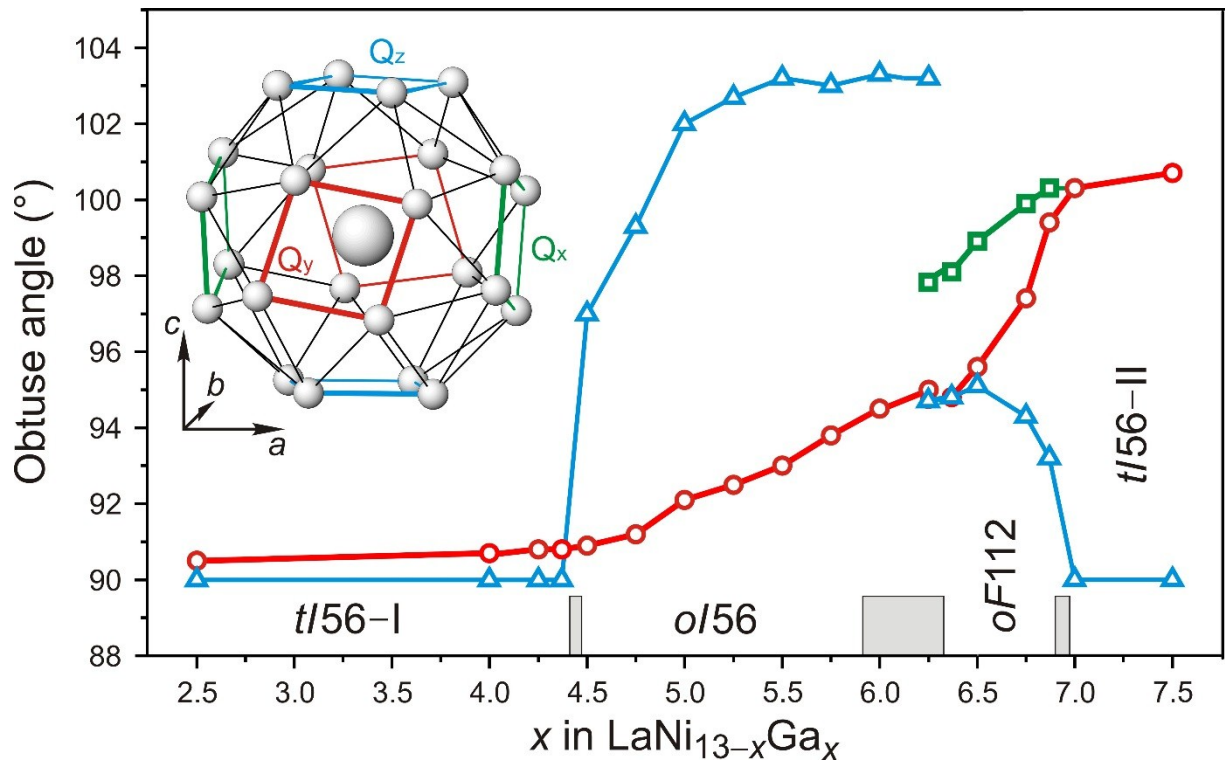


Figure S3. Deformation of the coordination polyhedron of the La position (snub cube) in $\text{LaNi}_{13-x}\text{Ga}_x$ series. Rhombic distortion (obtuse angle) of the initially quadratic faces of snub cubes is used as a measure of the deformation.

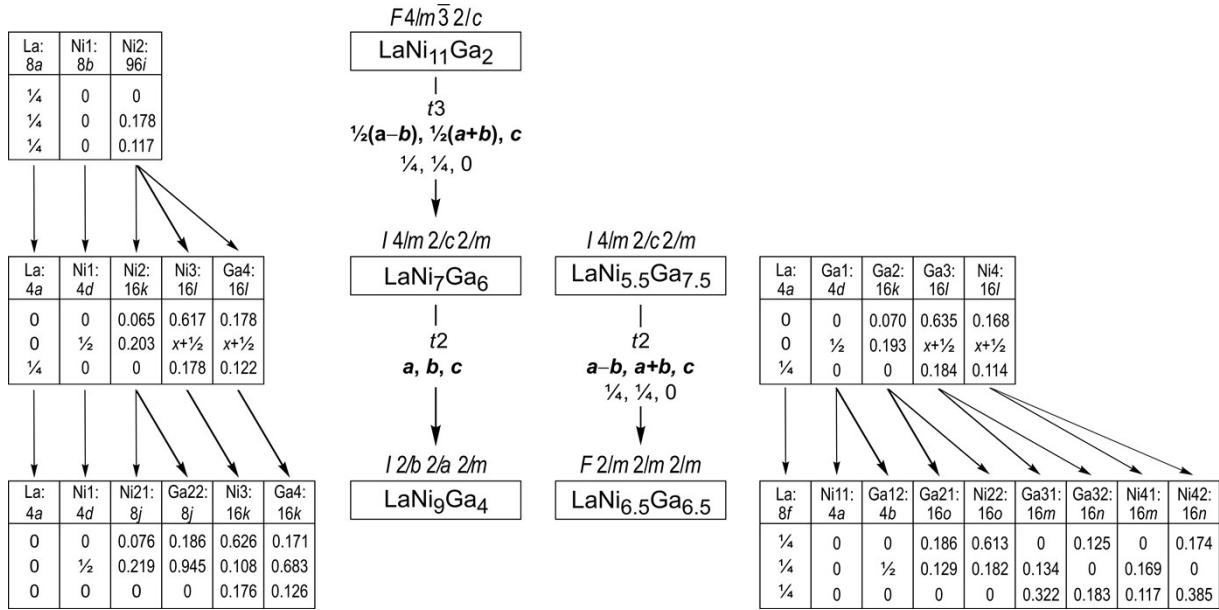


Figure S4. Group-subgroup relations in the Bärninghausen formalism for the four NaZn_{13} -related types of structure observed in the $\text{LaNi}_{13-x}\text{Ga}_x$ and $\text{CeNi}_{13-x}\text{Ga}_x$ series, which are presented on the basis of the La system. The indices of the *translationsgleiche* (t) transitions and the unit cell transformations are given.

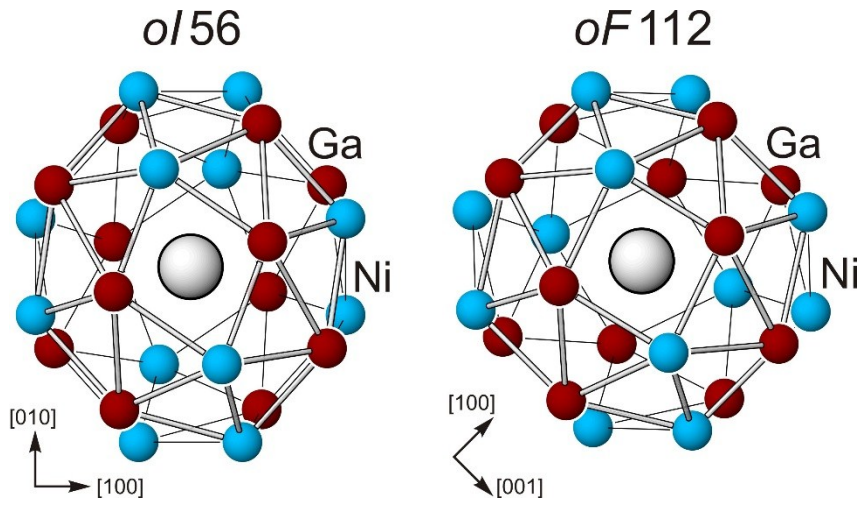


Figure S5. Coordination polyhedra around La atoms in the structures *oI56* and *oF112* projected along [001] and [010], respectively.

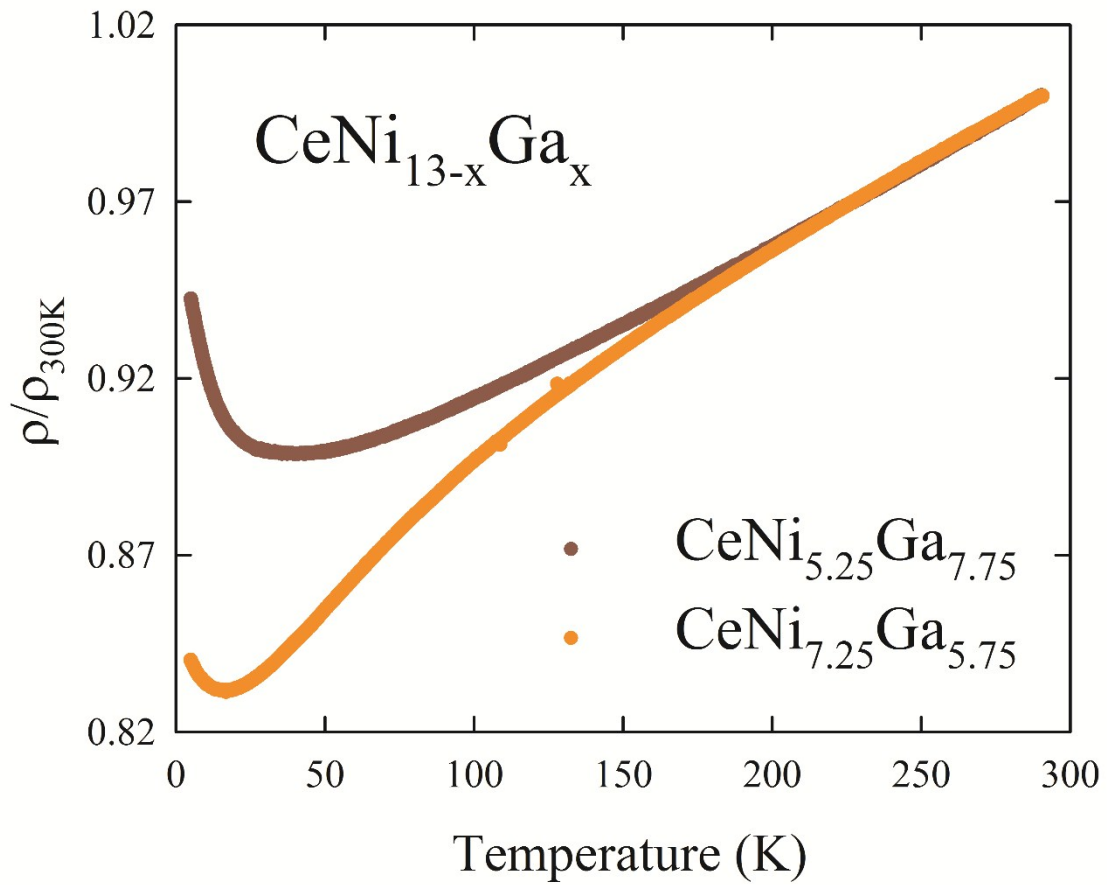


Figure S6. Temperature dependencies of the reduced electrical resistivity of two selected alloys from the $\text{CeNi}_{13-x}\text{Ga}_x$ series, i.e. $\text{CeNi}_{5.25}\text{Ga}_{7.75}$ (upper curve) and $\text{CeNi}_{7.25}\text{Ga}_{5.75}$ (lower curve).